Experimental and Numerical Investigation on the Strengthening IPE Steel Column with Welded Steel Plates under Axial Load

Mostafa I. Mostafa[1], Nabil S. Mahmoud[2], Fikry A. Salem[3]

[1]B. Sc., Demonstrator, Civil Engineering department, Faculty of Engineering, Mansoura University
[2] Professor, Structural Engineering Dept., Faculty of Engineering, Mansoura University
[3]Assoc. Professor, Structural Engineering Dept., Faculty of Engineering, Mansoura University

Abstract:- It is possible to repair the I-shape steel columns in many historic bridges by welding steel plates to their flanges. However, after the column's reinforcing plates have been welded to them, welding residual stresses, initial imperfections and column load can all have a major impact on the strength of the column. A nominal axial resistance is the target for the steel column. The steel column won't be able to support the intended applied load under different conditions, such as changing the building's use from residential to public or storage (additional live loads), and strengthening is thus necessary. Only a few experimental studies on the strengthening of steel columns with welded cover plates are currently available In order to evaluate the strength behavior of strengthening steel columns using steel plates welded parallel to the flange, either parallel to the web or parallel to the flanges and the web combined, this paper provides an experimental and numerical investigation. Twelve specimens were tested using full-scale testing to determine the failure mechanisms, development of stresses, and load-deformation. Every column that was tested had an IPE160 section with a different length. The program ABAQUS/standard v. 6.13 was used to operate the finite element model. Theoretical models correctly predicted the axial load-carrying capacity of the plate-strengthened columns under axially compression loading, as shown by a comparison of the theoretical and experimental data.

Key words:- *Strengthening, Steel Columns Cover Plate, Experimental, Axial Load, Finite Element Model, Initial Imperfection.*

I. INTRODUCTION

Steel is an iron-carbon alloy that may be used alone or in combination with other materials. Carbon may make up to 2.1% of the weight of steel. Due to its high strength and good ductility, ease of manufacturing, relative affordability, and status as the ideal recyclable material, it is quite popular.[1].

Compressive members, like columns, are essential structural elements because they carry and distribute the majority of the building's lateral and vertical stresses. In essence, no column can support loads at its maximum capacity without buckling. They may fail under axial compression depending on the application because of structural instabilities like overall/local buckling. Short columns often collapse by material crushing and local buckling, whereas long columns typically fail by overall buckling. The load bearing capacity of columns are greatly influenced by their slenderness and length[2].

A structure collapsing under an axial compressive stress is referred to as buckling behavior. The thin structural components that support the axial compressive loads are known as columns. A column may fail due to structural instability known as buckling if the compressive load is too great. Consequently, the issue of steel columns buckling is a major one. Negative outcomes or unjustified safety factors might occur from underestimating this influence.[3].

Building constructions are supported by columns, thus when a column behaves poorly, the entire structure might collapse. Column buckling in constructions has been the cause of several accidents. In the design of new steel structures and in the maintenance of existing ones, preventing the overall buckling of steel components in compression is a major challenge. Therefore, strengthening the columns in a building is an essential component. Rehabilitation falls into two broad categories: strengthening and repair. The strengthening category will be the main focus of this investigation. Strengthening is the process of bringing a structural component that is not damaged up to a predetermined level from its existing capability [4].

One of the most important issues in this field of structural engineering is the retrofitting of existing structures. Retrofitting of old structures is thought to be necessary due to causes including poor structure design or construction, alterations to load specifications, changes in structural function, the steel rusting and being exposed to impact or fire [5-6]. Numerous investigations on reinforced steel columns using various strengthening techniques have been carried out recently. Numerous methods, such as the usage of FRP (fiber-reinforced polymer) plates, can be used to create them[7-9], concrete filling of steel columns [10], concrete jacketing [11-12] and welded steel plates [13] have been investigated. Due to its ease of use and cost-effectiveness, applying steel reinforcement sheets has emerged as one of the most common methods for retrofitting steel columns [14]. When a column has been loaded with dead loads and partly

live loads after a structure have been put into operation, it may be essential to reinforce compression members. The process of welding or attaching cover plates to steel compression members is frequently used for reinforcement. Despite the fact that numerous structures have been strengthened, There hasn't been a lot of research done on reinforced steel columns. The design procedure usually involves overlapping the stress before reinforcement to the stress imposed after reinforcing the column in order to ensure that the stress in the rolled form does not exceed yield.For short columns, this method is straightforward and conservative, but it is unclear how intermediate and thin columns would behave after reinforcement [15]. Using a new numerical analytical model that derives the compressive resistance from ideas of equilibrium, compatibility, and force-deformation connections, Shek and Bartlett have studied the behavior of wide-flange columns reinforced with cover plates parallel to flanges. The original W shape's and the new cover plates' yield strengths, as well as additional factors like start out-of-straightness and end eccentricity, were examined. It was demonstrated that locked-in dead-load stresses had no discernible impact on either the strong or weak axis compressive capacity of a reinforced W shape column when the slenderness ratio (kL/r) is between 33 and 90. The capacity decreases as locked-in dead load pressures increase for slenderness ratios between these limitations [16]. Although Shek and Bartlett's work offers some relevant information on the behavior and using existing column curves for the design of reinforced steel columns wasn't advised while designing the columns out of steel[16]. Additionally, Shek and Bartlett's analysis only looked at columns reinforced parallel to flanges and neglected to take into account the impact of welding residual stress originating from welding of the cover plates[16].

According to a review of the literature, there have been very few experiments on steel columns reinforced with welded steel plates. Consequently, a nonlinear finite element (FE) model was created in order to expand the small database of test results and to examine the whole range of factors not included in the experiments. First, test results were compared to the performance of the FE model. Several characteristics thought to have an impact on the strength of reinforced steel columns were examined using the validated model.

In this paper, a series of experiments that look at loading IPE steel columns and loading reinforced IPE steel columns with steel cover plates welded either parallel to the web, parallel to the flanges, or parallel to the web and the flanges together in the third midspan of the column length, will be described. Additionally, an accurate finite element method (FEM) model that takes into account the orientation of the steel plates and suitable material constitutive models were produced using the commercial software ABAQUS [17]. To ensure the offered models are accurate, the behavior, ultimate strengths, and failure mechanisms are predicted and compared with the results of the experiments. Since it is expected that the reinforced IPE160 section already satisfies the local buckling requirement and that the reinforcing plates will be proportioned to satisfy that requirement, local buckling was not particularly taken into account. Although local buckling might have been permitted by the numerical investigation's mesh's level of refinement, it was not noted in the research. Additionally, experimental testing will be used to study the reinforced specimen's axial compression behavior. Finally, finite element analysis (FEA) will be performed to identify the buckling behavior, and then a straightforward design will only be used at and close to the weld.

II. EXPERIMENTS

The test program, which was carried out, is described in this part and comprises detailed material property testing and tests on columns. Thereafter, the results will be discussed and the test setup for the columns provided. The failure modes will next be discussed in wide detail.

A. Material Characteristics

➤ Tensile Coupon Tests

To assess the stress-strain characteristics of the steel column under tension, three 35 and 40 mm tensile coupons made from virgin steel plate were tested in an Instron uniaxial testing system. Table 1 contains important details about these test coupons. A mean value of 246 N/mm^2 for the yield stress was found after three testing. Although testing showed a rise in stress after yielding, it is believed that high-strength steel lacks a clearly defined strain-hardening area. The material's mean ultimate stress under tension was found to be 360.8 N/mm^2, despite this. In Fig. 1, stress-strain diagrams are shown. Fig. 2 illustrates the tensile coupons' machine and mode of failure.

Table 1 Tests of Tensile Coupon.

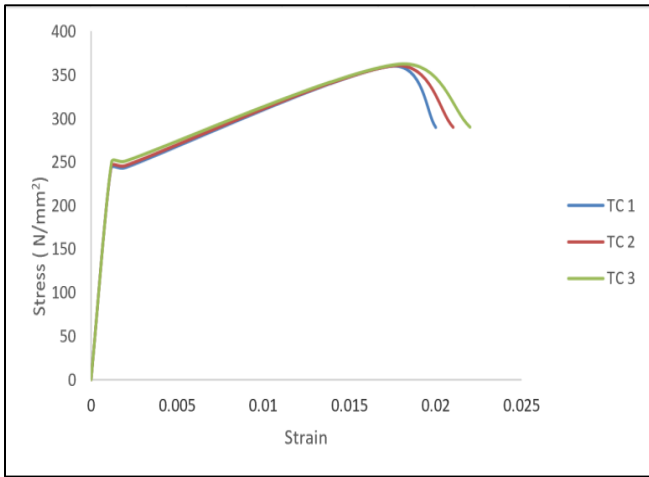| 3	Specimen number	Yield stress, f_y (N/mm^2)	Ultimate stress, σ_u (N/mm^2)	Young's modulus, Es (N/mm^2)	Yield strain ($\mu\varepsilon$)
A	TC 1	243	360.1	210,000	1157
B	TC 2	245	360.4	210,000	1166
C	TC 3	250	362	210,000	1190
	Mean	246	360.83	210,000	1171

Fig 1 Tests of Tensile Coupon .

Fig 2 Tensile Coupon Machine and Typical Failure Mode.

B. Testing Series

Twelve IPE steel columns were evaluated in this investigation, nine of which were IPE-strengthened (A2-A4, B2-B4, and C2-C4), and three of which served as control specimens (A1, B1, and C1). The columns were all (1.5 m, 2.0 m and 2.5m) long respectively using IPE160 steel sections (Fig.3) with fixed -pin ended conditions. A list of test specimens and parameters is presented in Table 2.

➤ Geometry of Specimens

IPE160-cross-section columns (A2 and B2) are covered by two 500-mm-long web plates in the middle third of the column's length. IPE160 cross-section columns (A3 and B3) are covered by two 500 mm-long flange plates at the midway point of the column's length. Columns (A4 and B4) having a cross section of IPE160 are covered by four plates, each 500 mm long, two of which are web plates and two of which are flange plates, at the midway point of the column's length. At the third middle of the column's length, a column (C2) with a cross section of IPE160 is covered by two web plates that are 830 mm long. A column (C3) with an IPE160 cross section is covered by two 830 mm-long flange plates at the middle of the column's length. A column (C4) with an IPE160 cross section is covered by four plates, each 830 mm long and made up of two web plates and two flange plates. Using 5 mm throat-thick longitudinal fillet welds along the whole length of the plates, the steel plates were all joined with the columns.

$E_s = 210,000$ N/mm^2 was used as the steel's elastic modulus, and $v_s = 0.30$ as the steel's Poisson's ratio.
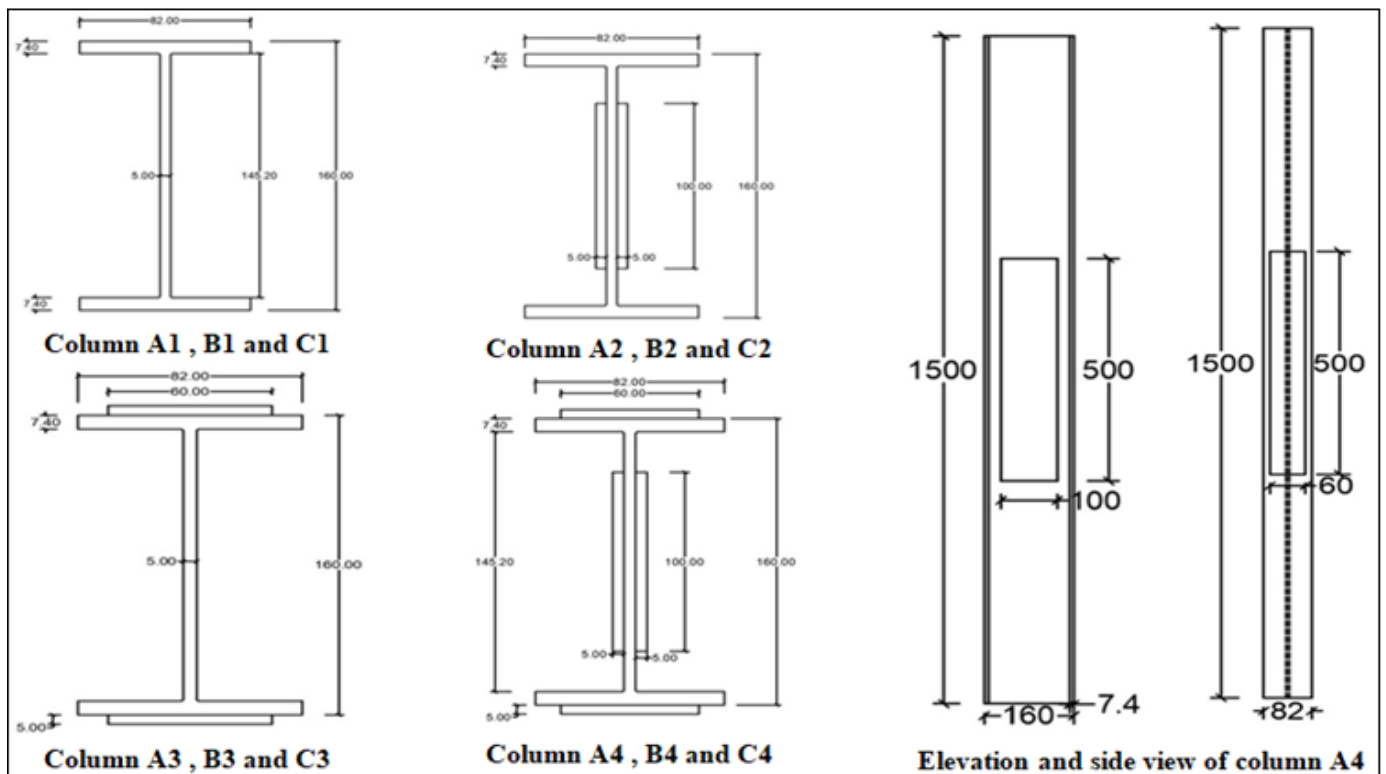
Fig 3 Column Tests Details.

www.ijisrt.com

C. Experimental Setup

The steel structure illustrated in Fig. 4 was utilized for the experimental work for this study at the University of Mansoura's Heavy Structures Lab. To approach consistent compression, massive, thick steel plates were used at both ends of the plaster-cast columns. Column specimens are fixed at the machine frame base and tested under an axial compression force as part of the axial load test procedures. The weight at the top of the column was applied using a digital hydraulic jack with a 1000kN capability. Both the loaded column top and the fixed column base were in place. The whole displacement to failure was seen by testing all columns under displacement control. In Fig. 5, the test setup, strain gauges, and strain indicator are presented. The stresses at the most important places of the columns were measured using electrical resistance of a 60 mm length strain. As shown in Fig. 5, the displacement at the column's midpoint was measured using dial gauges.

Fig 4 Main Test Machine
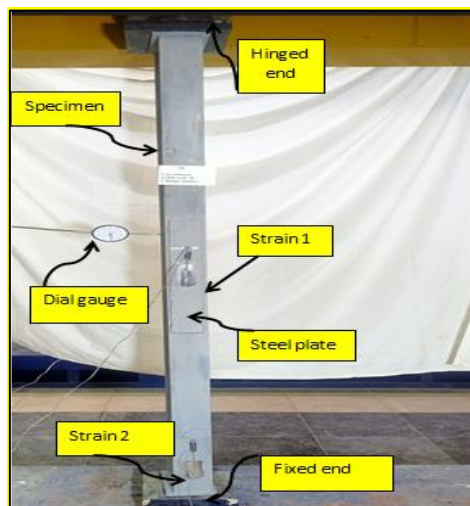
Fig 5 Test Set Up.

➤ *Test Procedure*

Test Methodology, Each column experienced axial compression testing with a 50kN force. A digital hydraulic jack with a 1000kN capacity was used to apply the cyclic load at the top of the column.

Table 2 Experimental Series

groups	specimen	Height (L),mm	Cross section	Plate Dimensions,(mm)	orientation of plates
A	A1	1500	IPE160	-	-
	A2	1500	IPE160	2pl 100*5	web
	A3	1500	IPE160	2pl 60*5	flange
	A4	1500	IPE160	2pl 100*5 & 2pl 60*5	web& flange
B	B1	2000	IPE160	-	-
	B2	2000	IPE160	2pl 100*5	web
	B3	2000	IPE160	2pl 60*5	flange
	B4	2000	IPE160	2pl 100*5 & 2pl 60*5	Web& flange
C	C1	2500	IPE160	-	-
	C2	2500	IPE160	2pl 100*5	web
	C3	2500	IPE160	2pl 60*5	flange
	C4	2500	IPE160	2pl 100*5 & 2pl 60*5	Web& flange

III. EXPERIMENTAL RESULTS

A. Failure Loads

Table 3 provides an overview of the test findings for Specimens A2-A4, B2-B4, and C2-C4 in terms of the maximum loads attained for each specimen and the % increase in strength from strengthening steel plates compared to the control equivalents. The table also includes the failure mechanisms, strain at ultimate load at the specimen's outermost surface, and lateral displacement at ultimate load. Depending on the various factors examined, the gains in axial strength usually ranged from 4.84 to 19.15%. This increase in axial strength results from the steel's plates' ability to increase cross-sectional flexural rigidity (EI), which in turn delays the beginning of global buckling.

B. Load–Axial Displacement

Figs. 6a, 6b, and 6c show the load-axial displacement responses for each group. Figures (7a, 7b, and 7c) show all of the load-lateral displacement curves that were calculated.

C. Load–Strain

For each group, the load-average strain curves were plotted and are displayed collectively in Figs. (8a, 8b, and 8c). At the loading end, the axial displacement data are recorded. Before the peak load occurs, the curves often exhibit a sharp initial response. The incidence of global buckling is typically correlated with the ultimate load. The figures show that adding steel reinforcement does not appreciably change the initial axial stiffness despite increasing the ultimate load. This is shown by the only marginally higher slope of the curves when compared to control specimens.
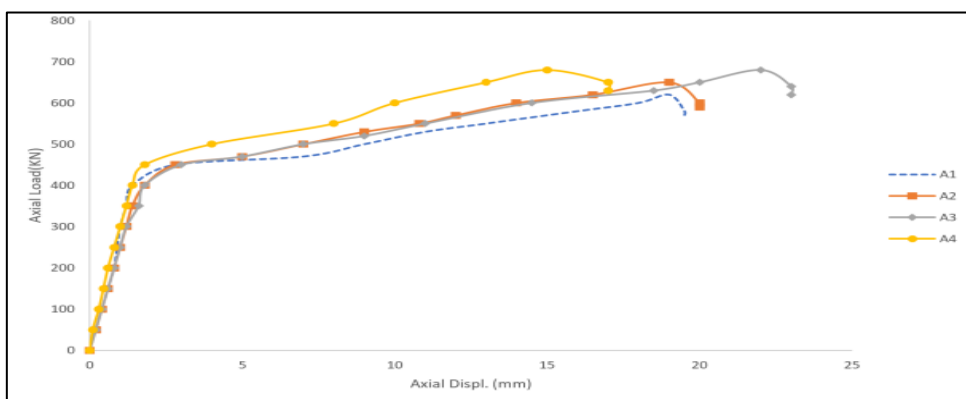
(a)
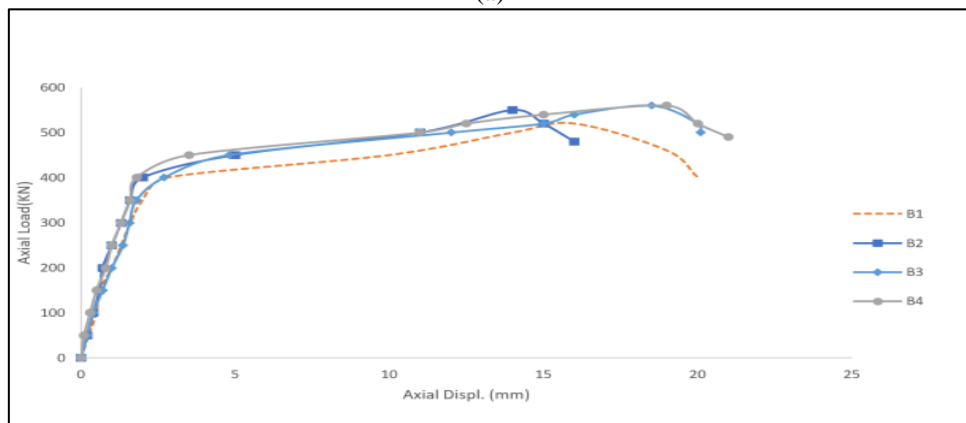
(b)
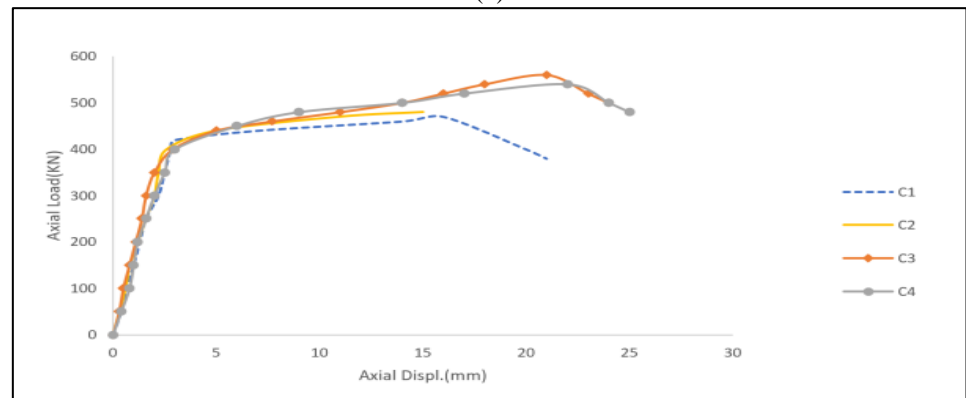
(c)

Fig 6 Load–Axial Shortening Curves (a) Group A, (b) Group B and (c) Group C.
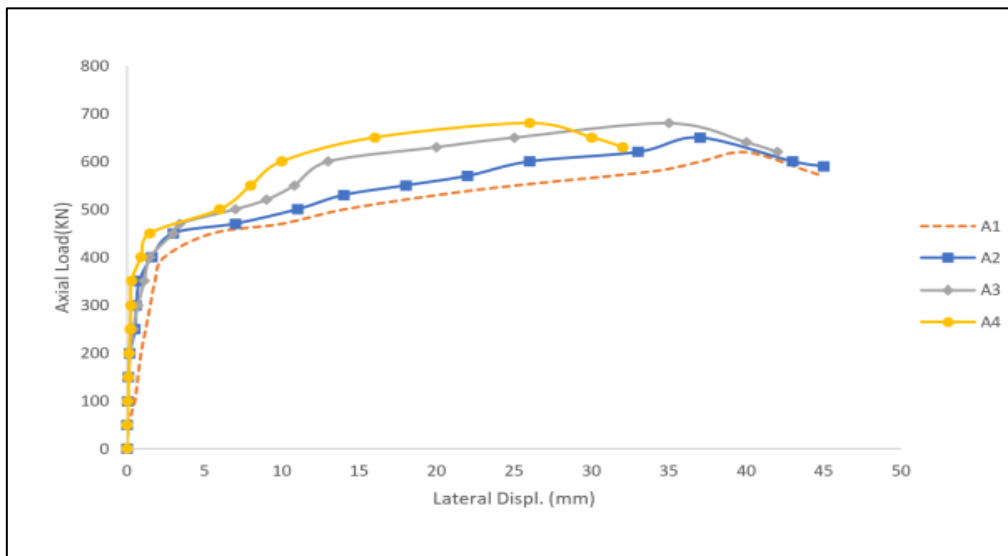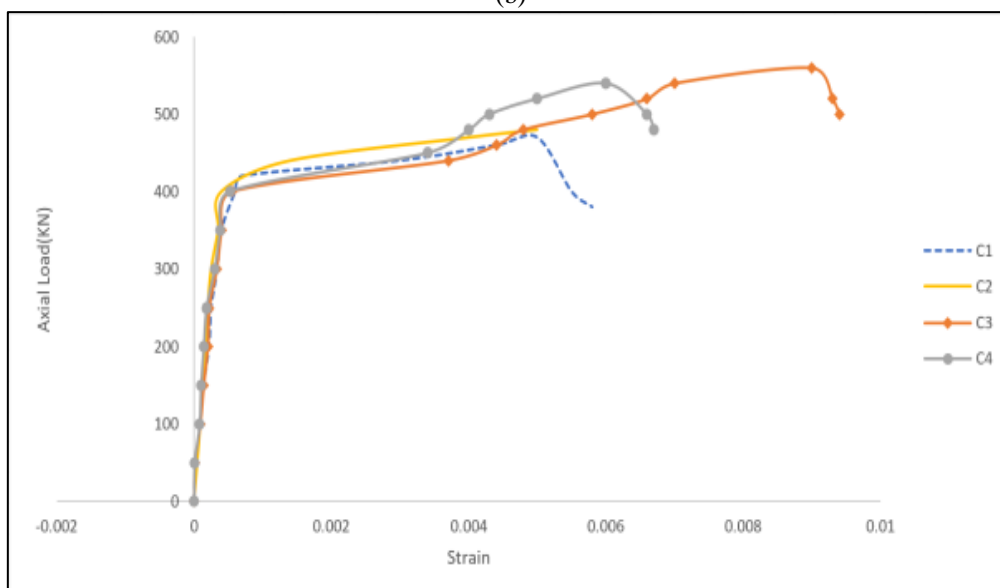
(a)
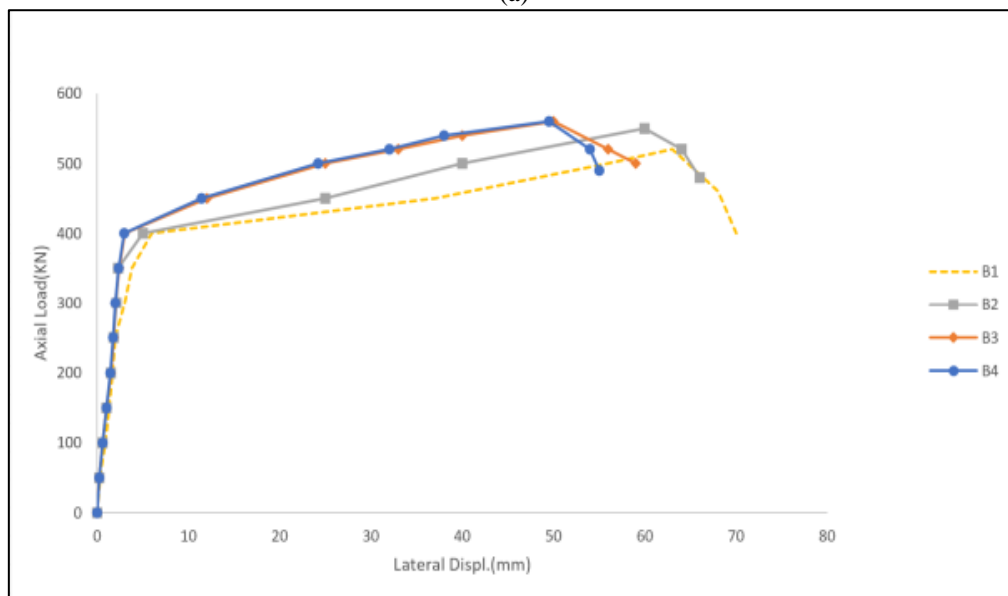
(b)
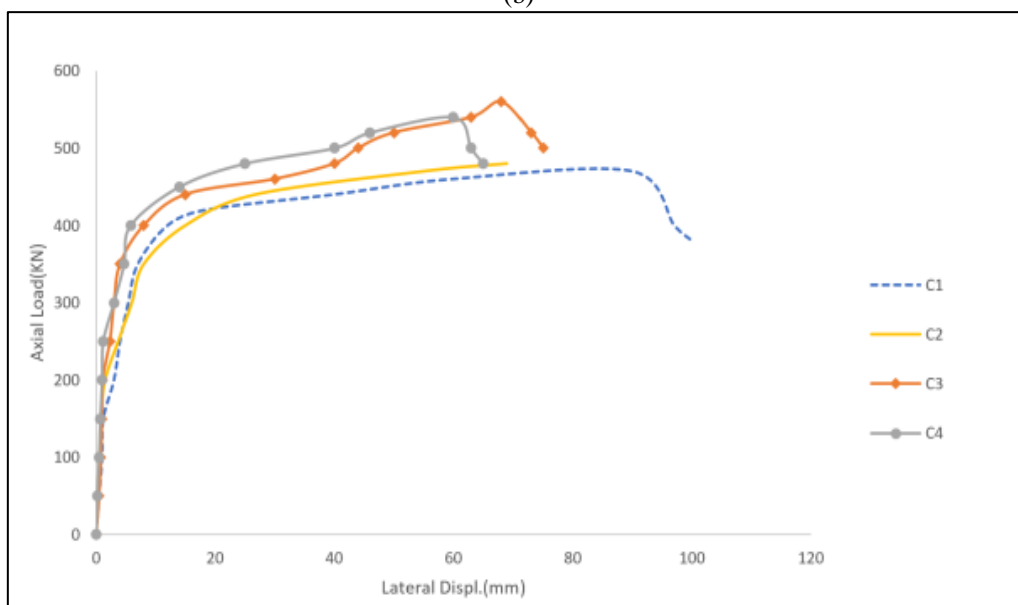
(c)

Fig 7 Load–Lateral Displacement Curves a) Group A, (b) Group B and (c) Group C.
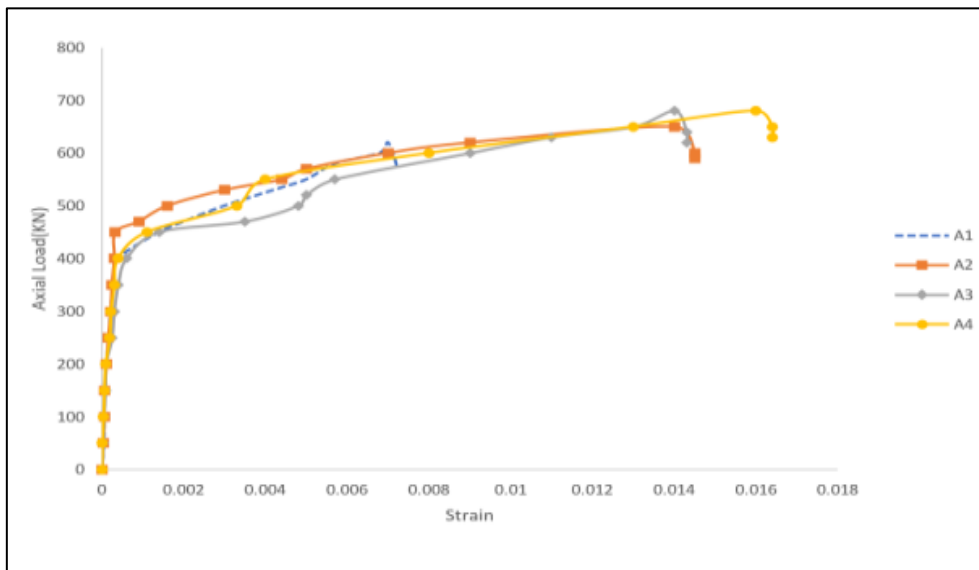
(a)
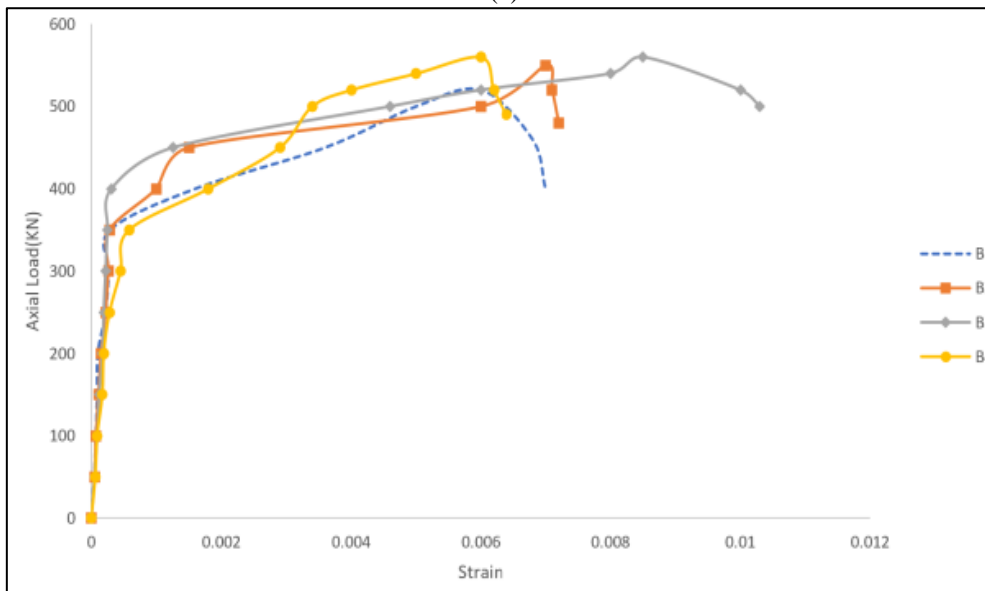
(b)

(c)

Fig 8 a) Group A, b) Group B, and c) Group C Load-Strain Curves.

D. Maximum Lateral Displacements

➤ *For Steel Columns Group A*

The maximum lateral displacement (MLD), of steel columns are represented in table 3, The MLD of column A2 is lower than column A1 by about 7.5% at failure, The MLD of column A3 is lower than column A1 by about 14.29% at failure and, The MLD of column A4 is lower than column A1 by about 40% at failure As shown in Fig.9.
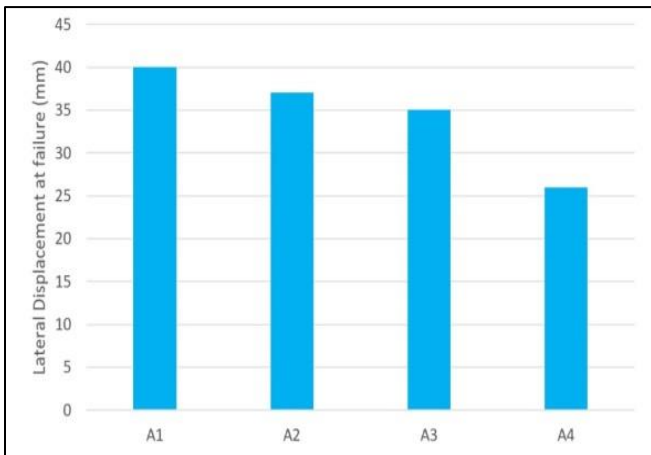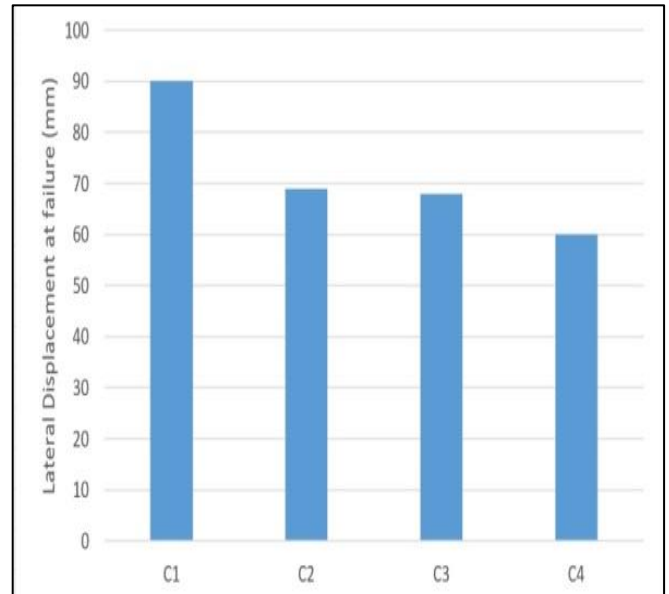

Fig 9 Recorded the Maximum Lateral Displacement at Failure for Group A.

➤ *For Steel Columns Group B*

The maximum lateral displacement (MLD), of steel columns are represented in table 3, The MLD of column B2 is lower than column A1 by about 5% at failure, The MLD of column B3 is lower than column A1 by about 21.67% at failure and The MLD of column B4 is lower than column A1 by about 22.5% at failure As shown in Fig.10.
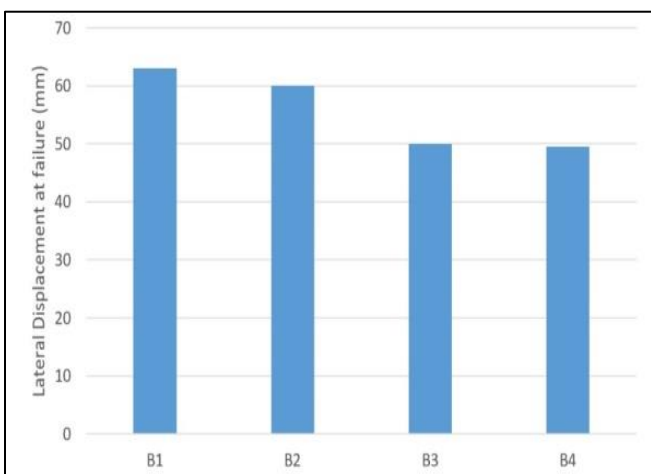
Fig 10 the Greatest Lateral Displacement at Failure for Group B

➤ *For Steel Columns Group C*

The maximum lateral displacement (MLD), of steel columns are represented in table 3, The MLD of column C2 is lower than column A1 by about 23.33% at failure, The MLD of column C3 is lower than column A1 by about 24.24% at failure and, The MLD of column C4 is lower than column A1 by about 33.33% at failure As shown in Fig.11.

Fig 11 Recorded the Maximum Lateral Displacement at Failure for Group C.

E. Maximum Axial Loads

➤ *For Steel Columns Group A*

The maximum axial load (MAD), of steel columns are represented in table 3, The MAD of column A2 is greater than column A1 by about 4.84% at failure, The MAD of column A3 is greater than column A1 by about 9.7% at failure and, The MAD of column A4 is greater than column A1 by about 9.7% at failure As shown in Fig.12.
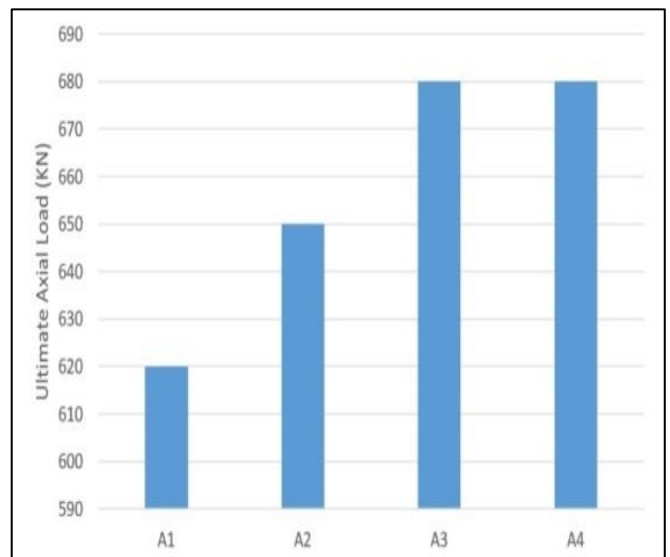

Fig 12 Recorded the Maximum Axial Load at Failure for Group A.

➤ *For Steel Columns Group B*

The maximum axial load (MAD), of steel columns are represented in table 3, The MAD of column B2 is greater than column B1 by about 5.8% at failure, The MAD of column B3 is greater than column B1 by about 7.7% at failure and, The MAD of column B4 is greater than column B1 by about 7.7% at failure As shown in Fig.13.
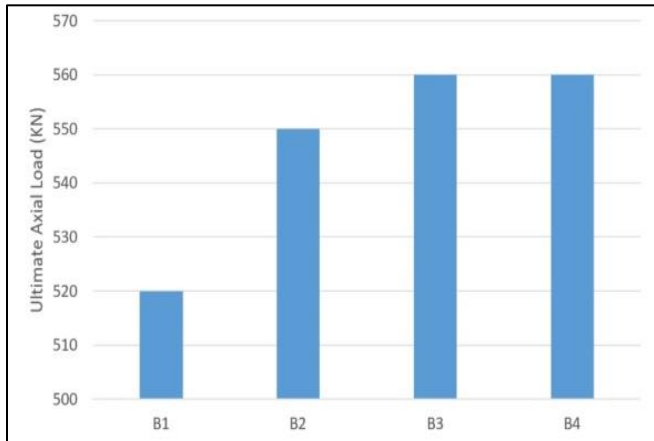
Fig 13 Recorded the Maximum Axial Load at Failure for Group B.

➢ *For Steel Columns Group C*

The maximum axial load (MAD), of steel columns are represented in table 3, The MAD of column C2 is greater than column C1 by about 2.13% at failure, The MAD of column C3 is greater than column C1 by about 19.15% at failure and, The MAD of column C4 is greater than column C1 by about 14.9% at failure As shown in Fig.14.
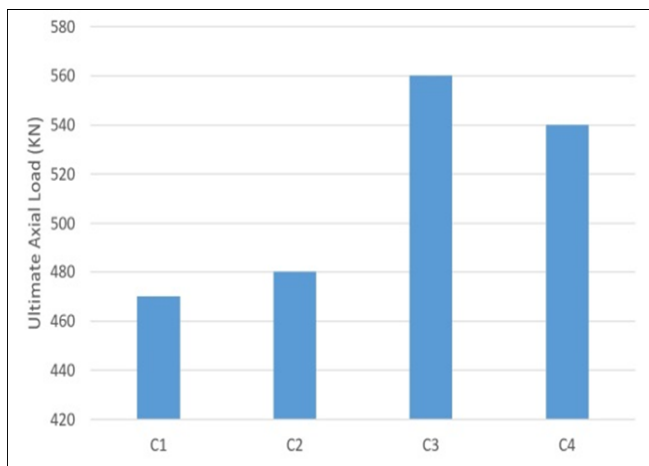

Fig 14 Recorded the Maximum Axial Load at Failure for Group C.

➢ *Curves of Axial Load Versus Column Displacement*

The curves of axial load against lateral displacement for all examined specimens are shown in Figs.15 to 26 for steel columns.
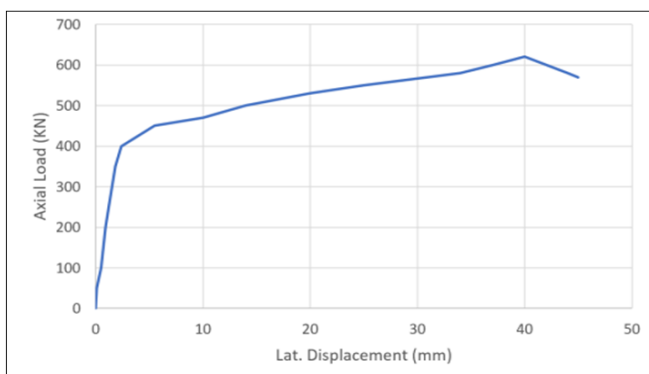
Fig 15 Column A1's Load-Displacement.
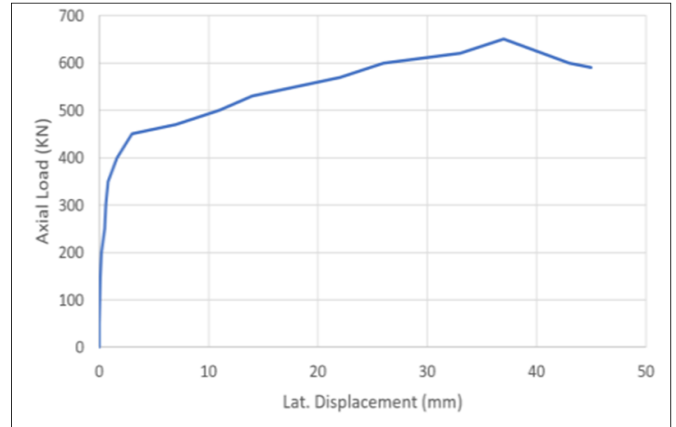
Fig 16 Column A2's Load-Displacement.
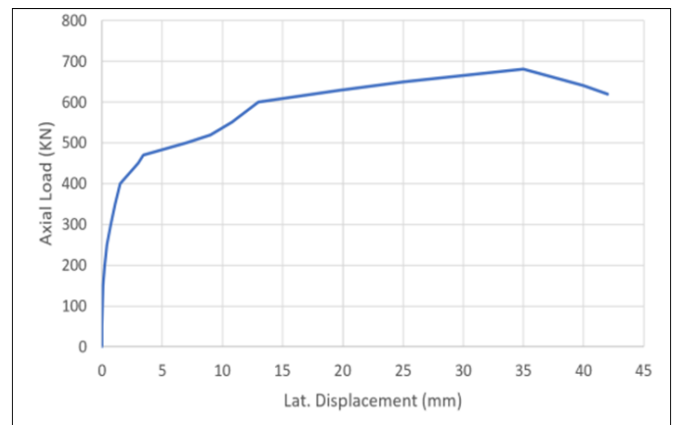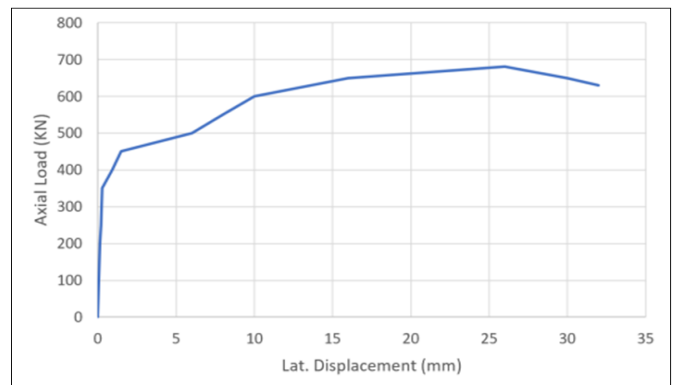

Fig 17 Column A3's Load-Displacement.

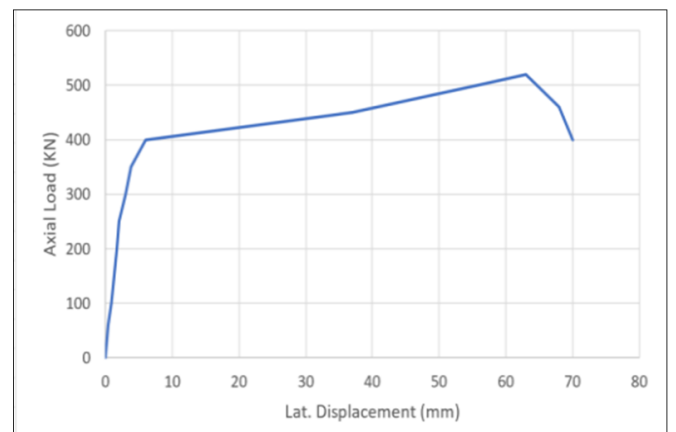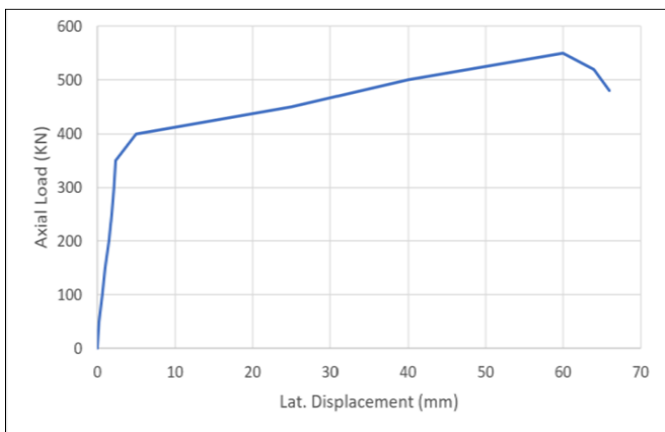Fig 18 Column A4's Load-Displacement.

Fig 19 Column B1's Load-Displacement.

Fig 20 Column B2's Load-Displacement.

Fig 21 Column B3's Load-Displacement.

Fig 22 Column B4's Load-Displacement.
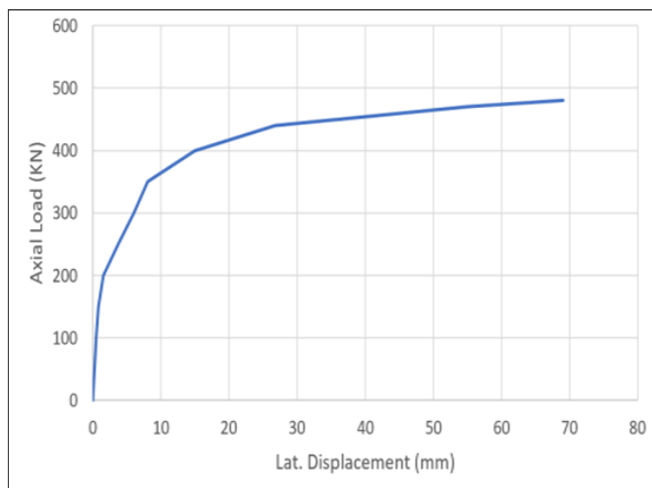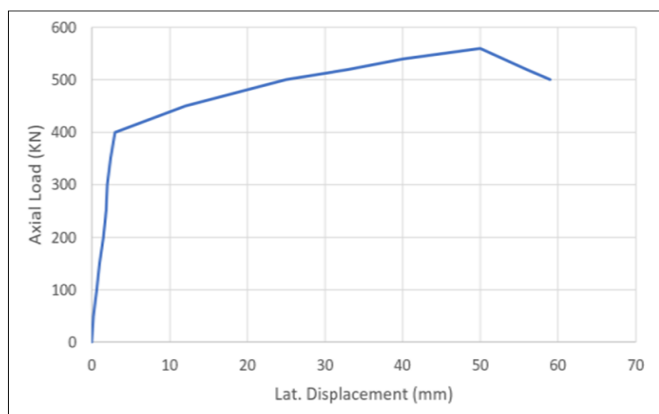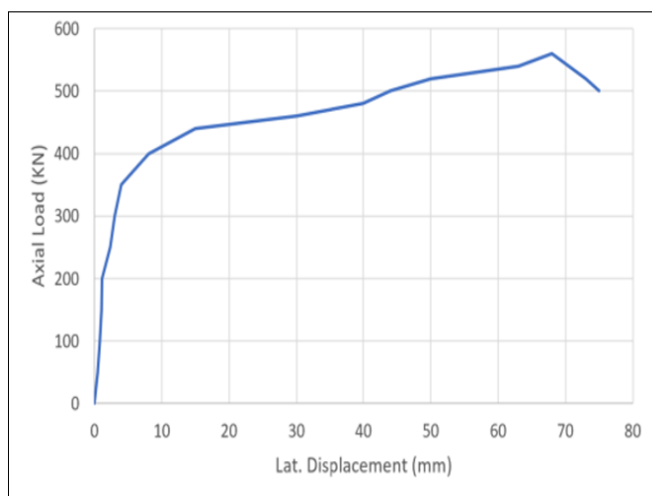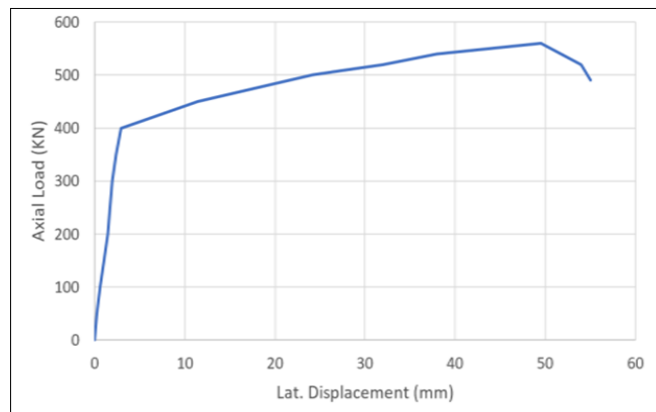

Fig 23 Column C1's Load-Displacement.

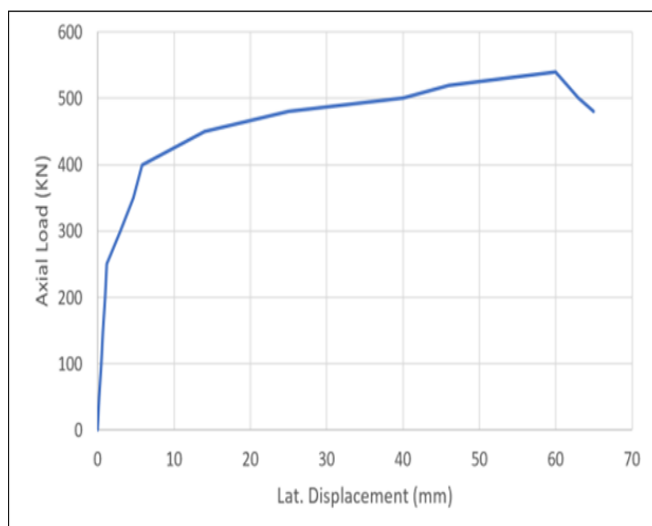Fig 24 Column C2's Load-Displacement.
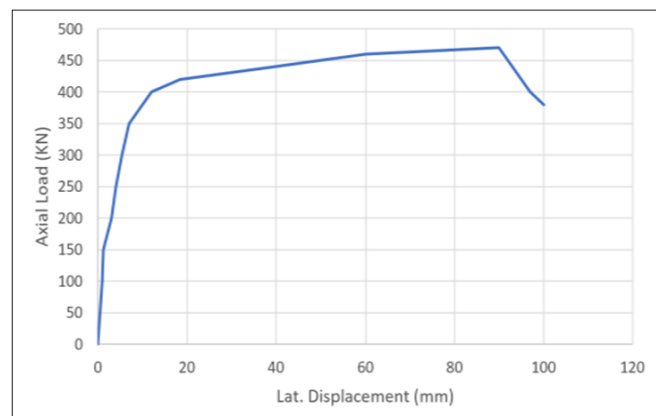

Fig 25 Column C3's Load-Displacement.

Fig 26 Column C4's load-displacement.

F. Failure Modes

Due to the fixed pin-ended column's characteristic global buckling, all three control specimens collapsed in the same way. Similar globally buckling was also experienced by all reinforced specimens Fig. 27.
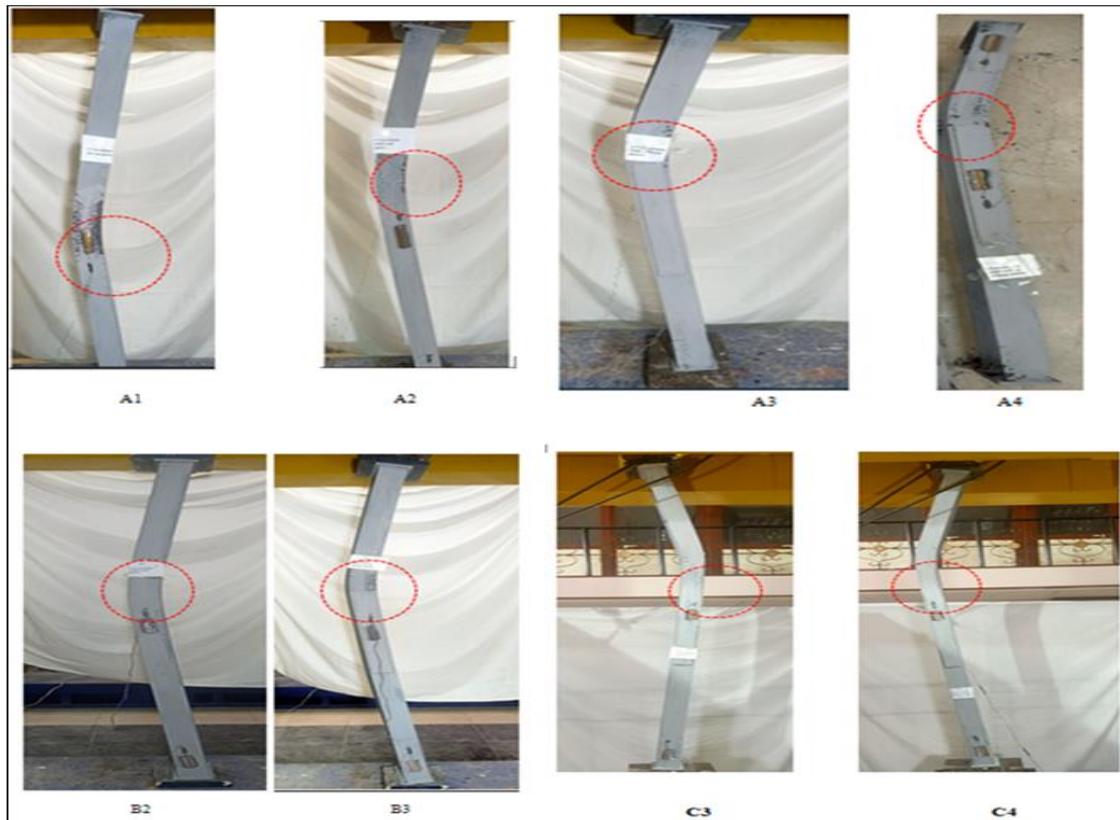
Fig 27 (A1, A2, A3, A4, B2, B3, C3, C4) Failure Shape of Tested Columns.

Table 3 conclusions of Column Test Results.

groups	specimen	Length (mm)	class	$P_{u,exp}$ (KN)	Percent Gain in strength	Lateral displacement at ultimate load(mm)	Strain at ultimate load(ε)	Failure mode	Failure position
A	A1	1500	compact	620	control	40	0.0072	Global buckling (GB)	Mid third
	A2	1500	compact	650	4.84	37	0.0145	GB	Top third
	A3	1500	compact	680	9.70	35	0.0143	GB	Top third
	A4	1500	compact	680	9.70	26	0.0164	GB	Top third
B	B1	2000	compact	520	control	63	0.007	GB	Mid third
	B2	2000	compact	550	5.80	60	0.0072	GB	Top third
	B3	2000	compact	560	7.70	50	0.0103	GB	Top third
	B4	2000	compact	560	7.70	49.50	0.0064	GB	Top third
C	C1	2500	compact	470	control	90	0.0058	GB	Mid third
	C2	2500	compact	480	2.13	69	0.005	GB	Mid third
	C3	2500	compact	560	19.15	68	0.0094	GB	Top third
	C4	2500	compact	540	14.90	60	0.0067	GB	Top third

IV. GENERATION OF A FINITE ELEMENT MODEL

A. Method of Finite Element

The behavior of the strengthening IPE steel columns under axial load is described in this section along with a discussion of the finite element modeling techniques employed. In structural analysis, Finite Element modeling is becoming more important and common due to the accuracy of the results and the savings in time and money that can be obtained through FE modeling.

Usually, structural components are numerically analyzed using the finite element method [18]. In this study,

a reinforced steel column finite element model was developed and validated. ABAQUS, a for-profit finite element program, was used to create the finite element model [17]. In order to explore all possible cross sections for reinforced columns, three groups of finite element models were examined: columns with strengthening plates parallel to the web, columns with strengthening plates parallel to the flanges, and columns with strengthening plates parallel to the web and flanges together. Fig. 28 depicts an example meshed model with different restrictions that was created using FEM.

B. Development of Finite Element Model

The three elements that make up the finite element model of a reinforced column are the rolled section, the

strengthening plates, and the connections between the strengthening plates and the rolled section. The rolling section and reinforcing plates were discretized using element S4R from the ABAQUS finite element library. The six degrees of freedom per node, four-node, doubly curved, general-purpose solid element S4R can tolerate finite stresses. The welded connection between the reinforcing plates and the rolled section was modeled using merge.

To properly represent the residual stress pattern, enough elements had to be employed to build the cross-section, and the aspect ratio of the elements had to be kept below 4.0 to avoid any potential numerical problems. These two factors determined the mesh size used to model the reinforced columns.

All of the components of the reinforced columns were designed using an isotropic, elastic strain hardening plastic material. The yield stress was set at 245 MPa for all steel components, and the Poisson's ratio was calculated using data from a coupon test to be 0.3. The global imperfection size was estimated to be 1/500 of the column's whole length at the mid height section, whereas the local imperfection was assumed to be 0.1 t.

Finally, using fixed pin-ended supports, the boundary conditions of the finite element model are implemented. Referring to Figure 29, the reference points "RP-1" and "RP-2" are subject to boundary constraints and loading, and their degrees of freedom are related to those of the edge nodes lying at the top and bottom of the column. Various researchers have utilized this strategy to simulate boundary conditions in numerical analysis [19] . At the bottom of the column, rotation around axes and translation in the x, y, and z directions are forbidden. Because there is unrestricted vertical translation along the longitudinal axis, translation in the z direction is not prohibited at the top loaded portion of the column. Loading is applied as a central concentrated vertical force at the top of the column in a load step that is divided into a number of sub-steps in order to provide an accurate solution. In the investigations, a minimum load increase of 1E-5 of the applied load is used.
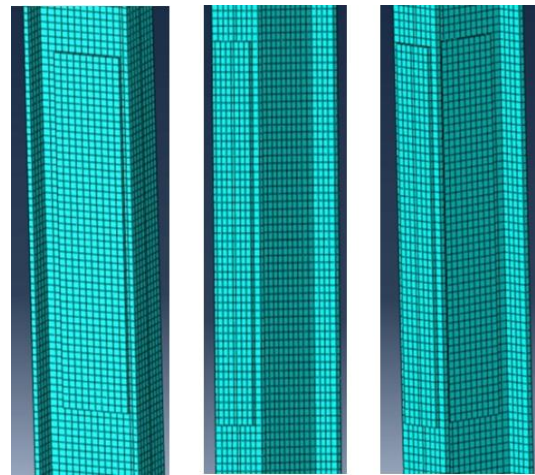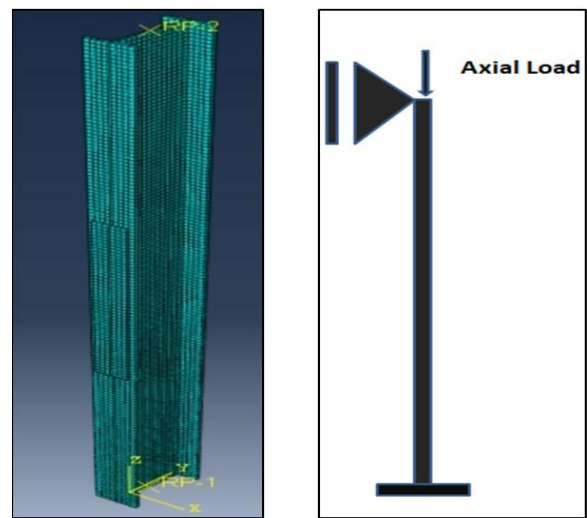

Fig 28 Meshed Models

Fig 29 Conditions for Loading and Boundaries.

C. Comparison of Results from Finite Element Models

This section compares the results of experiments on steel columns conducted using experimental (EXP) data and finite element model (FEM) results. Axial load capability of all steel columns is compared. Results from the experimental data are presented in table 4, and the outcomes of the finite element model are contrasted with them.

Table 4 Experimental vs Analysis Results

specimen	Experimental results		Analysis results		Exp./Analysis
	Failure load (KN)	Lateral displacement(mm)	Failure load (KN)	Lateral displacement(mm)	
A1	620	40	617	44.1	1.005
A2	650	37	652.7	41	0.996
A3	680	35	652	39.4	1.043
A4	680	26	660	37	1.031
B1	520	63	562	71.1	0.925
B2	550	60	597.6	65.8	0.92
B3	560	50	591.5	58.3	0.947
B4	560	49.5	609.7	56	0.918
C1	470	90	511.6	105.5	0.918
C2	480	69	578.1	49.5	0.83
C3	560	68	564.4	81.5	0.992
C4	540	60	578	69.68	0.934
Mean					0.9549

➢ *Curves of Axial Load Versus Column Displacement*

Figs. 30 to 41 show a load-displacement graphic from the examination of the IPE steel columns. Compare the outcomes of the calculations made using the ABAQUS finite element program with those from the IPE steel columns tests to show the discrepancies. The results show that the finite element model and the experimental results of load displacement agree well, but there are a few small differences at the end of loading due to the test setup procedure and the FE model's lack of inclusion of a geometrical imperfection and the finite element and experimental results.
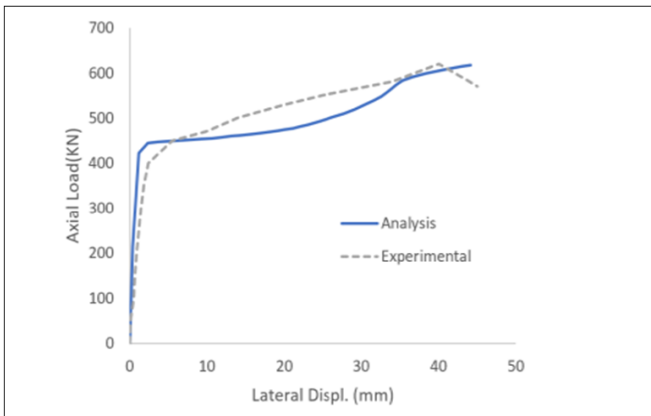

Fig 30 Analysis and Measurement Comparison of Column A1's Axial Load-Lateral Displacement Curves.
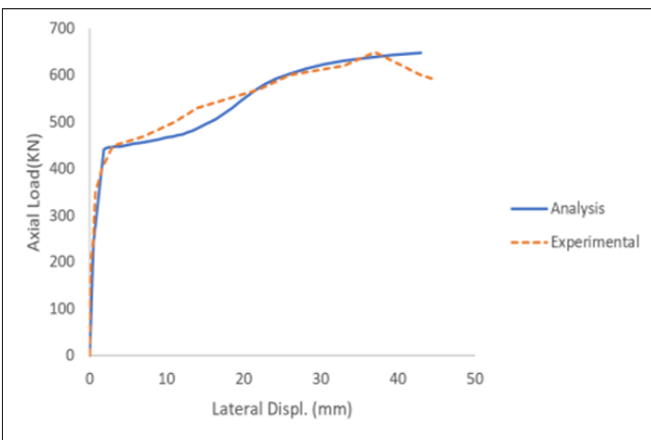

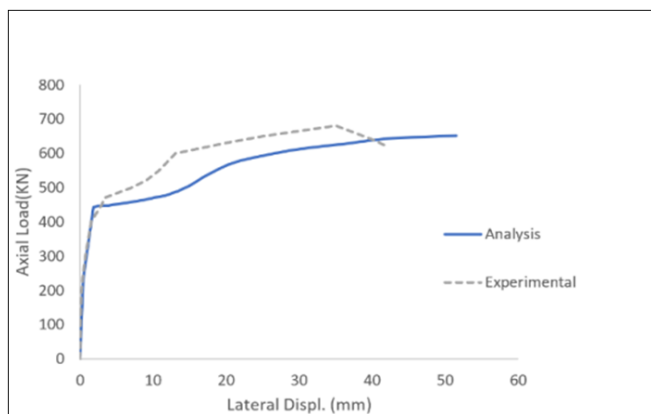Fig 31 Analysis and Measurement Comparison of Column A2's Axial Load-Lateral Displacement Curves.

Fig 32 Analysis and Measurement Comparison of Column A3's Axial Load-Lateral Displacement Curves.
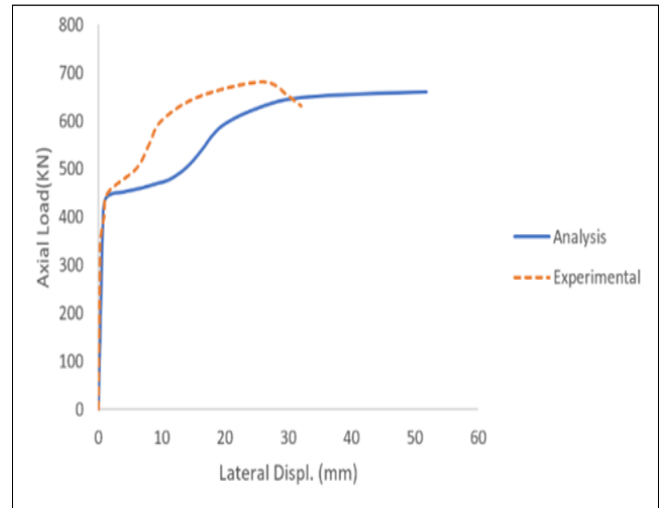

Fig 33 Comparison between Analysis and Measured Axial Load - Lateral Displacement Curves of Column A4.
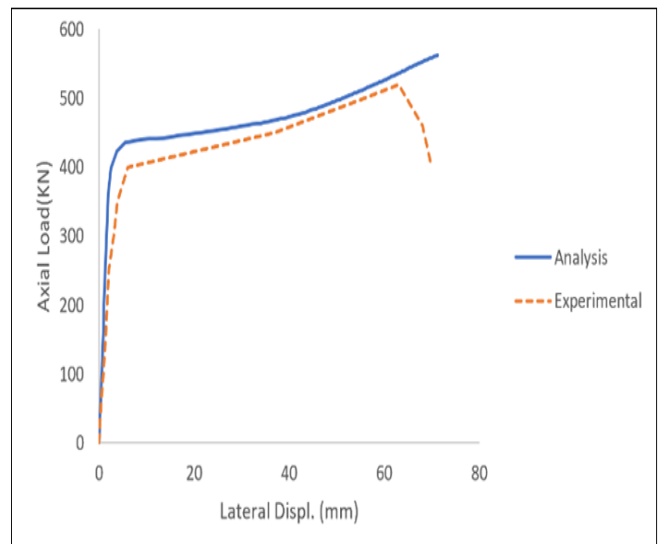

Fig 34 Analysis and Measurement Comparison of Column B1's Axial Load-Lateral Displacement Curves.
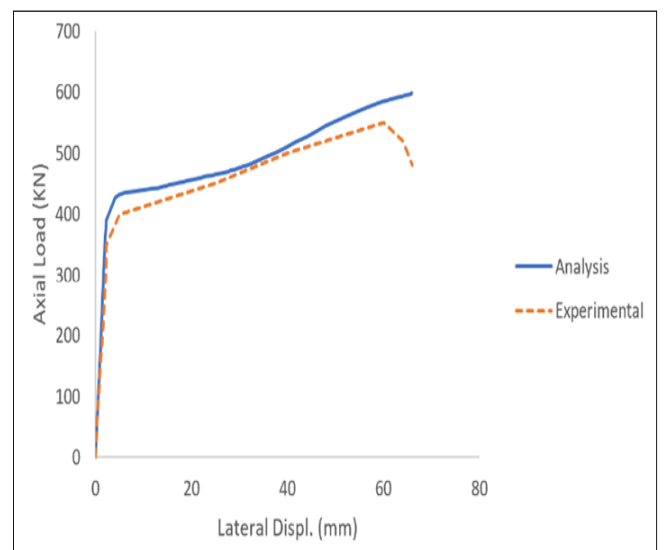

Fig 35 Analysis and Measurement Comparison of Column B2's Axial Load-Lateral Displacement Curves.

Fig 36 Analysis and Measurement Comparison of Column B3's Axial Load-Lateral Displacement Curves.

Fig 39 Analysis and Measurement Comparison of Column C2's Axial Load-Lateral Displacement Curves.
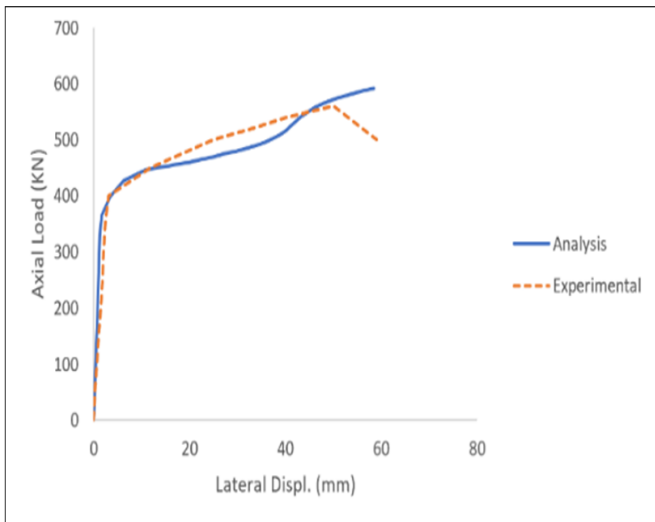

Fig 37 Analysis and Measurement Comparison of Column B4's Axial Load-Lateral Displacement Curves.
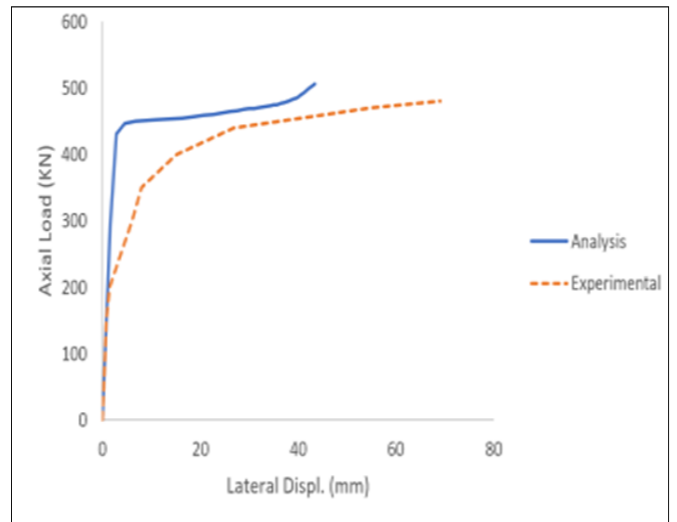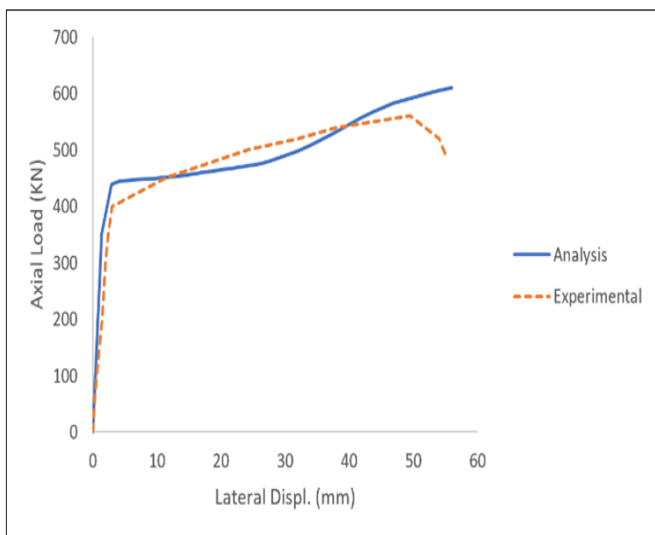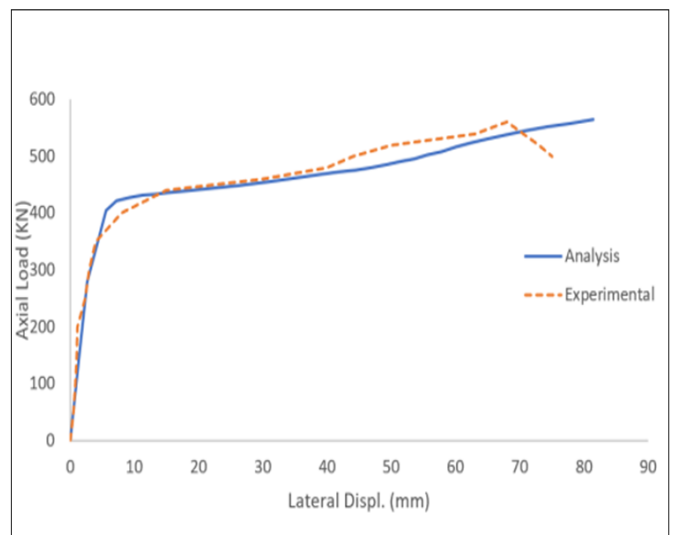

Fig 40 Analysis and Measurement Comparison of Column C3's axial Load-Lateral Displacement Curves.
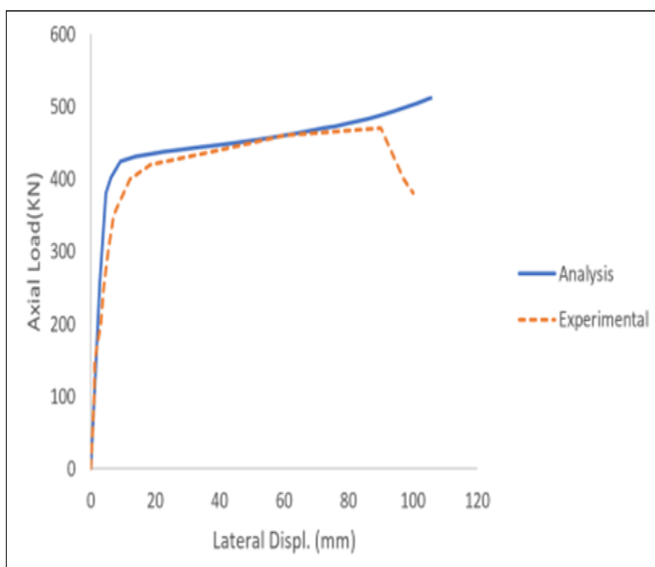

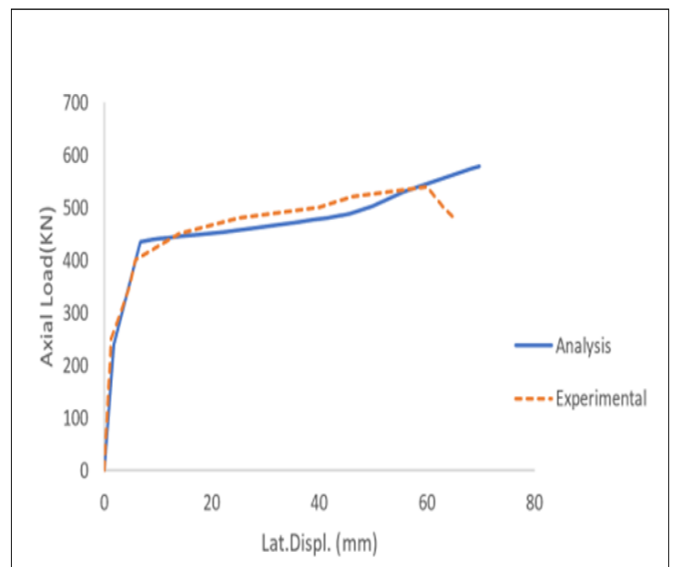Fig 38 Analysis and Measurement Comparison of Column C1's Axial Load-Lateral Displacement Curves.

Fig 41 Analysis and Measurement Comparison of Column C4's Axial Load-Lateral Displacement Curves.

V. CONCLUSION

The aim of this study was to strengthen IPE steel columns under axial stress using welded steel plates. Through a series of laboratory studies, the impact of the column length, the steel plates, and their orientation on the column behavior has been investigated. The test's results support the following assertion:

- The comparison values between ABAQUS and the experimental tests were very well understood. It is frequently believed that the FEM program can forecast how steel plate-strengthened columns would behave.
- The initial out-of-straightness has a significant influence on the strength and behavior of intermediate and long reinforced columns. The strength of reinforced columns decreases as the initial out-of-straightness rises.
- The study demonstrated that the behavior and strength of intermediate and long columns are significantly influenced by the interplay between the plate orientation and the buckling axis. For columns of identical slenderness reinforced by plates parallel to the web, the capacity of the column is larger when buckling occurs around the weak axis of the unreinforced portion.
- For columns of identical slenderness reinforced with plates parallel to the flange and the web and the flange together, the capacity is practically equivalent; nevertheless, at the start of the loading, reinforcing with the flange and web together was stiffer.
- Columns strengthened with welded flange steel plates consisting of an IPE160 section reinforced by two plates attached to flanges in the middle of the column's length have the maximum capability for carrying axial loads.
- The specimen (C2) exhibits the largest differences between experimental calculation and FEM due to the continuous welding of the steel plates with the web from two sides.

REFERENCES

[1]. L. Gardner, "The use of stainless steel in structures," *Prog. Struct. Eng. Mater.*, vol. 7, no. 2, pp. 45–55, 2005, doi: 10.1002/pse.190.

[2]. O. Yousefi, K. Narmashiri, A. A. Hedayat, and A. Karbakhsh, "Strengthening of corroded steel CHS columns under axial compressive loads using CFRP," *J. Constr. Steel Res.*, vol. 178, 2021, doi: 10.1016/j.jcsr.2020.106496.

[3]. M. Avcar, "Elastic Buckling of Steel Columns Under Axial Compression," *Am. J. Civ. Eng.*, vol. 2, no. 3, p. 102, 2014, doi: 10.11648/j.ajce.20140203.17.

[4]. H. M. Salman and M. H. Al-sherrawi, "Finite Element Modeling of a Reinforced Concrete Column Strengthened with Steel Jacket," pp. 916–925, 2018.

[5]. J. M. Adam and S. Ivorra, "Behaviour of axially loaded RC columns strengthened by steel angles and strips," no. October, 2007, doi: 10.12989/scs.2007.7.5.405.

[6]. K. C. G. Ong and J. H. Kang, "Jacketing of preloaded steel columns," *J. Constr. Steel Res.*, vol. 60, no. 1, pp. 109–124, 2004, doi: 10.1016/j.jcsr.2003.08.001.

[7]. M. R. Bambach, H. H. Jama, and M. Elchalakani, "Axial capacity and design of thin-walled steel SHS strengthened with CFRP," *Thin-Walled Struct.*, vol. 47, no. 10, pp. 1112–1121, 2009, doi: 10.1016/j.tws.2008.10.006.

[8]. J. Haedir and X. L. Zhao, "Design of short CFRP-reinforced steel tubular columns," *J. Constr. Steel Res.*, vol. 67, no. 3, pp. 497–509, 2011, doi: 10.1016/j.jcsr.2010.09.005.

[9]. S. Kalavagunta, S. Naganathan, and K. N. Bin Mustapha, "Proposal for design rules of axially loaded CFRP strengthened cold formed lipped channel steel sections," *Thin-Walled Struct.*, vol. 72, pp. 14–19, 2013, doi: 10.1016/j.tws.2013.06.006.

[10]. T. Y. Yang, D. P. Tung, and C. Xu, "Experimental and Analytical Evaluation of Concrete-Filled Crisscross Steel Tubular Columns Subjected to Earthquake Loads," *J. Perform. Constr. Facil.*, vol. 28, no. 6, 2014, doi: 10.1061/(asce)cf.1943-5509.0000551.

[11]. C.-S. Kim, H.-G. Park, K.-S. Chung, and I.-R. Choi, "Eccentric Axial Load Capacity of High-Strength Steel-Concrete Composite Columns of Various Sectional Shapes," *J. Struct. Eng.*, vol. 140, no. 4, 2014, doi: 10.1061/(asce)st.1943-541x.0000879.

[12]. C. Hui, W. Cao, Y. Wang, and B. Wang, "Experimental and simulation studies on the seismic performance of I-section steel-concrete composite columns," *Adv. Struct. Eng.*, vol. 18, no. 2, pp. 251–268, 2015, doi: 10.1260/1369-4332.18.2.251.

[13]. Z. Wu and G. Y. Grondin, "Behaviour of steel columns reinforced with welded steel plates," *Struct. Eng. Rep.*, no. 250, pp. 1–230, 2002.

[14]. Y. Liu and L. Gannon, "Finite element study of steel beams reinforced while under load," *Eng. Struct.*, vol. 31, no. 11, pp. 2630–2642, 2009, doi: 10.1016/j.engstruct.2009.06.011.

[15]. A. K. Bhowmick and G. Y. Grondin, "Limit state design of steel columns reinforced with welded steel plates," *Eng. Struct.*, vol. 114, pp. 48–60, 2016, doi: 10.1016/j.engstruct.2016.01.032.

[16]. K. K. W. Shek and F. M. Bartlett, "Analysis and design of rehabilitated built-up hybrid steel compression members," *Can. J. Civ. Eng.*, vol. 35, no. 12, pp. 1375–1387, 2008, doi: 10.1139/L08-077.

[17]. ABAQUS 6.13. "Abaqus Analysis User's Manual." Dassault Systèmes Simulia Core., Providence, RI (2013).

[18]. P. O. Awoyera, "Nonlinear finite element analysis of steel fibre-reinforced concrete beam under static loading," J. Eng. Sci. Technol., vol. 11, no. 12, pp. 1669–1677, 2016.

[19]. M. Longshithung Patton and K. Darunkumar Singh, "Buckling of fixed-ended lean duplex stainless steel hollow columns of square, L-, T-, and +-shaped sections under pure axial compression - A finite element study," *Thin-Walled Struct.*, vol. 63, pp. 106–116, 2013, doi: 10.1016/j.tws.2012.09.003.